# Use of interlacing mode measurements in the gyro-based attitude reconstruction software

Craig Stephenson

6 July 2015

# Contents

# 1 Introduction

For the creation of the star tracker attitude measurements, the current version of the gyro-based attitude reconstruction software uses at most nine star vector measurements, those found in positions 1–9 of the STR-specific diagnostics dataset, `AcmsDtmStr`. However, for the periods when interlacing mode was active, this dataset may contain measurements of up to 18 star vectors. The purpose of this note is to investigate how best to use the additional measurements.

When interlacing mode was active on-board, measurements were made on two consecutive ACMS cycles (frames), separated in time by 0.25 s. [2, p. 190] describes how the measurements from the earlier frame were propagated, using the estimated spacecraft rates, to the time associated with the later frame before being used to determine the attitude of the star tracker. The first question to be addressed is whether this propagation has been performed prior to writing the measurements to the `AcmsDtmStr` dataset or whether each row of data contains measurements made at two distinct epochs.

# 2 Timing investigation

To investigate the timing I have looked at the PACS scan map 1342254140. The advantage of using this observation is that there is a period of over 100 s (during the initial slew) when there are simultaneously (i) 18 star measurements; and (ii) the attitude of the spacecraft was changing rapidly ($\sim 325\ ''/\mathrm{s}$).[1] In addition, the attitude determination using either set of 9 stars is of good quality.[2] Figures 1 and 2 show the variation of the attitude (right ascension and declination) over this observation and Figures 3 and 4 show the quality of the attitude determination using the first (positions 1–9) and second (positions 10–18) set of star measurements respectively.[3]

The test performed consisted of comparing the attitude reconstructed using the first set of star measurements with that reconstructed using the second set of measurements when three different timing offsets, between the

[1] When the attitude of the spacecraft is fixed, the pointing reconstruction is insensitive to timing issues.

[2] In fact, each set contains a maximum of 9 stars. For most of the period under consideration this maximum is achieved.

[3] It is of some concern that for much of the period when interlacing mode was active, the stars in positions 1–9 were almost identical to those in positions 10–18 (see Section 4.3).

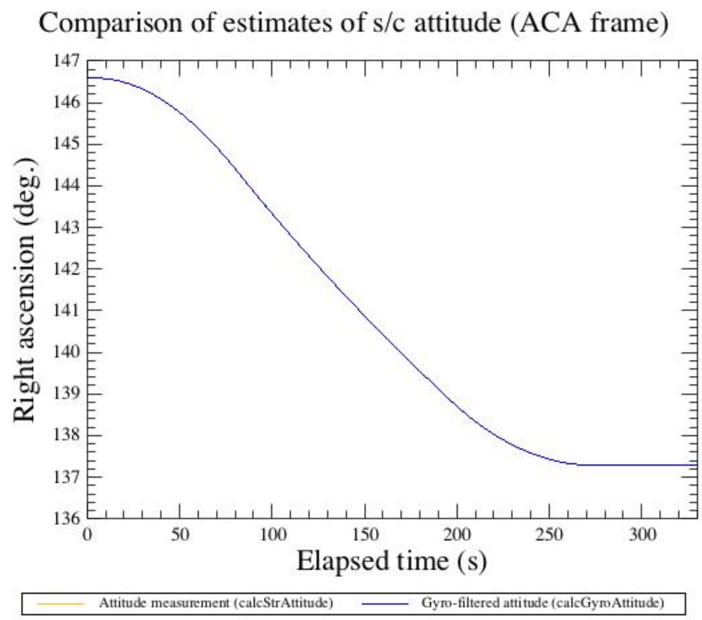


Figure 1: Right ascension (obs. 1342254140)

star tracker measurements and the gyro measurements, were applied to the second set: (a) `toff_star` = 0.189 (nominal), (b) `toff_star` = 0.439 (nominal + 0.25 s), and (c) `toff_star` = −0.061 (nominal − 0.25 s). The results are shown in Figures 5–7.[4] It is clear from the large biases seen in cases (b) and (c), particularly about the $z$-axis, that no additional timing offset needs to be introduced, i.e. all 18 star vector measurements in each row of `AcmsDtmStr` are associated with the same on-board time. (The differences in the attitude estimates for case (a) are consistent with the computed uncertainties; see Figures 8 and 9.)

[4] The rotations are from the attitudes reconstructed using the first set of star measurements to those reconstructed using the second set.

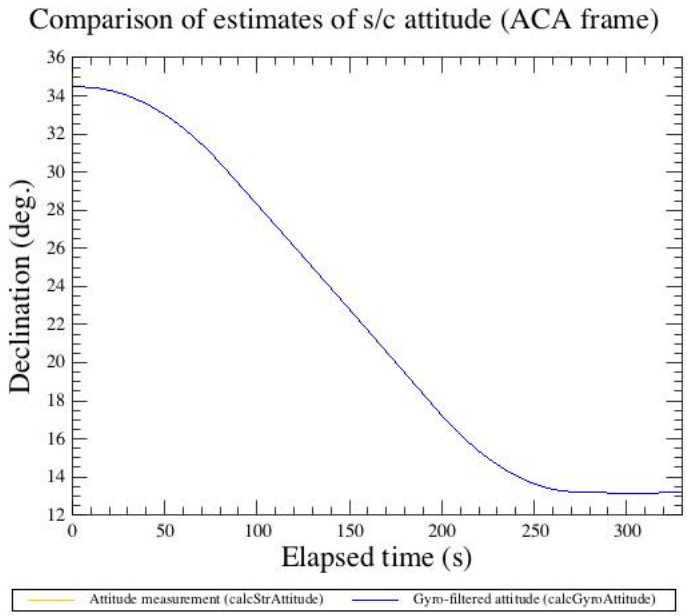


Figure 2: Declination (obs. 1342254140)

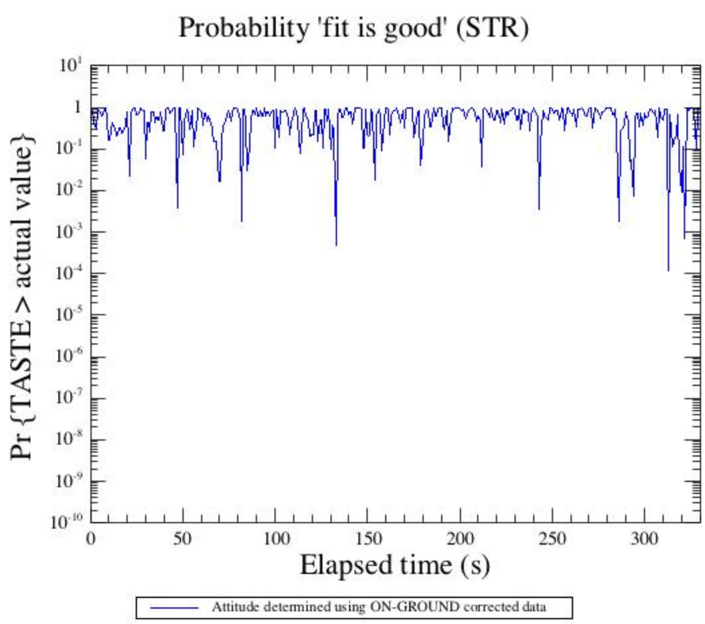


Figure 3: Attitude measurement quality (stars 1–9)

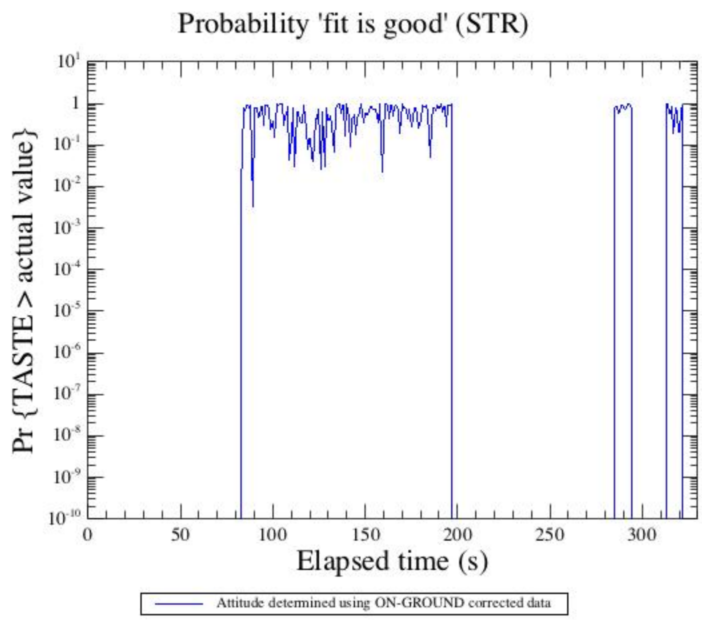


Figure 4: Attitude measurement quality (stars 10–18)

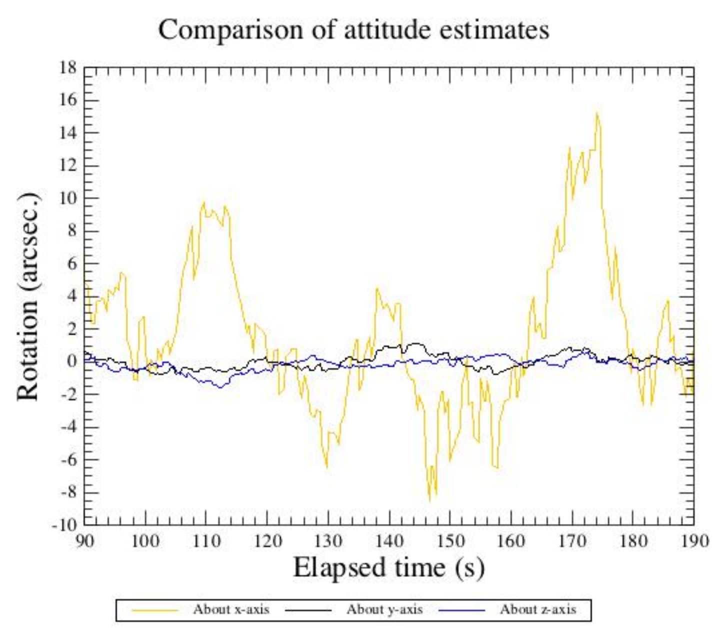


Figure 5: (a) `toff_star` = 0.189 (nominal)

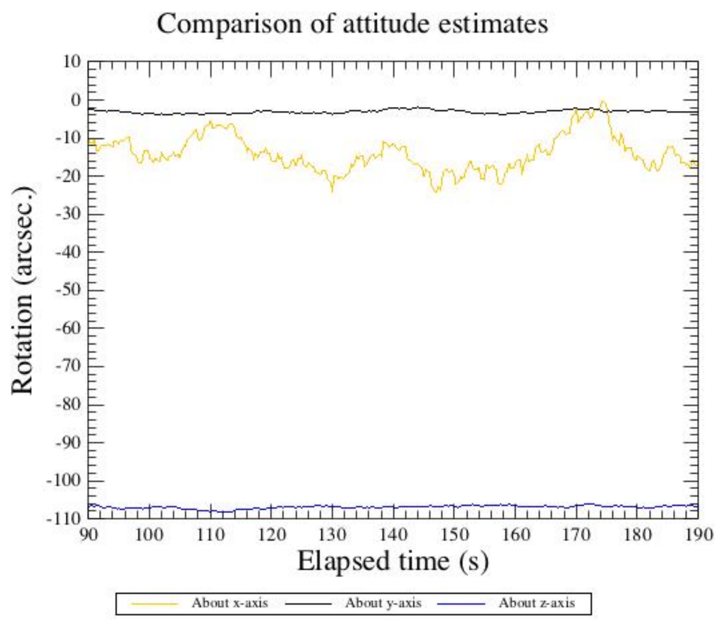


Figure 6: (b) `toff_star` = 0.439 (nominal + 0.25 s)

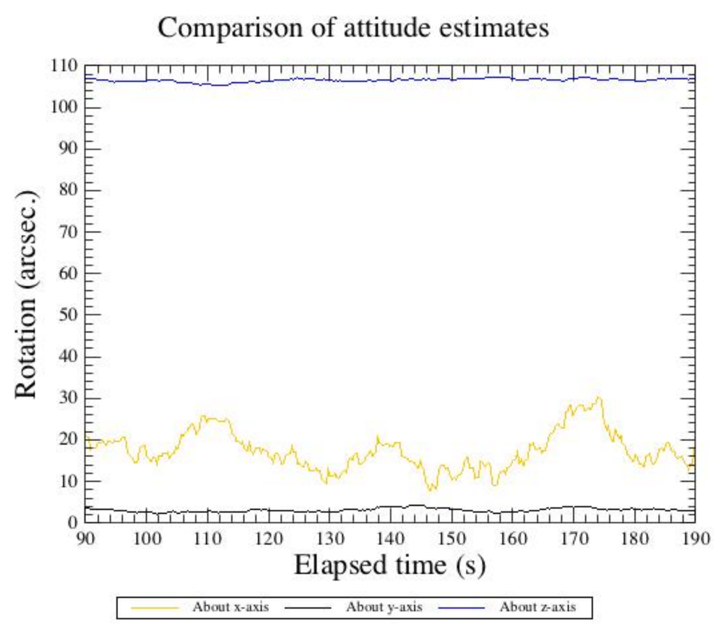


Figure 7: (c) `toff_star` = −0.061 (nominal − 0.25 s)

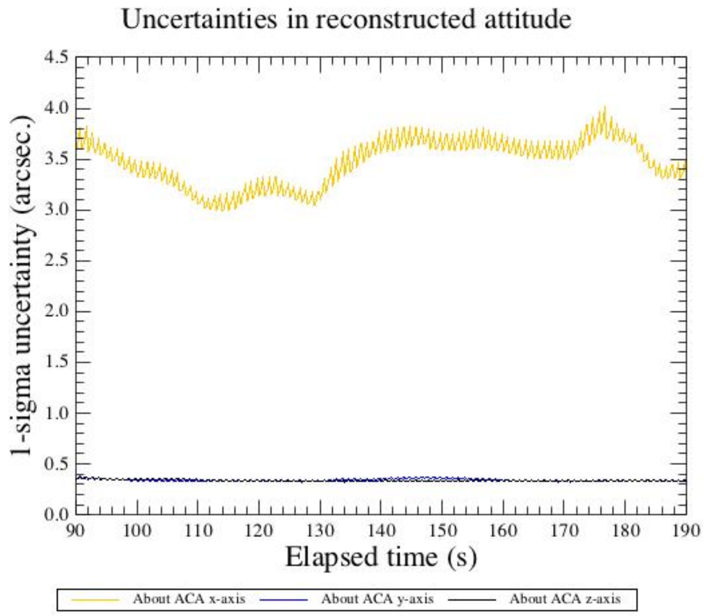


Figure 8: Uncertainties in reconstructed attitude (stars 1–9)

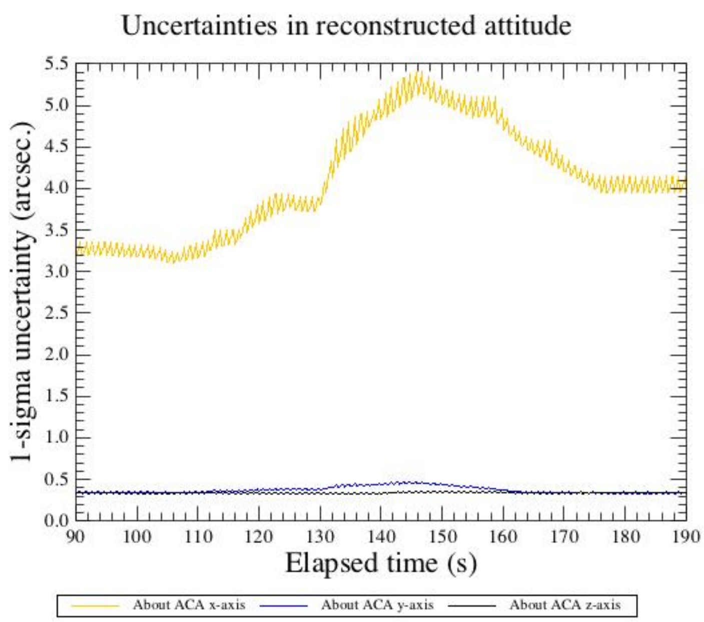


Figure 9: Uncertainties in reconstructed attitude (stars 10–18)

# 3 Back-propagation of measurements

The function `calcStrAttitude` creates improved star vector measurements (and from these improved attitude measurements) by removing the CCD distortion correction which was applied on-board and then applying an improved distortion correction [see 4, pp. 4–9]. Before performing this, any star vector measurements which have been propagated forwards by one ACMS cycle need first to be rotated back to where they were in the Boresight Reference Frame (BRF) at the time when they were made.[5]

So the next problem is to decide which of the two sets of star vector measurements came from the previous cycle. From the description given in the star tracker User Manual:

> In interlaced mode, the star information . . . of stars measured in the last cycle are *presented before* the star information measured in the previous cycle and updated to the current one. [2, p. 38]

it appears likely that it is measurements 1–9 which need to be back-propagated before performing the CCD distortion correction. If this were found to be true, then it would mean that the current implementation of `calcStrAttitude` is not correct, i.e. measurements 1–9 would need to be back-propagated (whenever interlacing mode was active) regardless of whether measurements 10–18 are used. (The creation of the residual distortion maps would also be affected by this need to back-propagate.)

However, as it is not entirely clear whether the above passage applies to the contents of the `AcmsDtmStr` dataset, a test was performed. All the

[5]Using the same notation as in [4], if $\mathbf{u}'_t$ is the (aberration-corrected) star vector at time $t$—here expressed as a quaternion—and $\hat{\omega}_x$, $\hat{\omega}_y$, $\hat{\omega}_z$, are the on-board estimated body rates (obtained from columns `estAngVelX`, `estAngVelY` and `estAngVelZ` of the `AcmsScmTM` dataset) then its direction $\Delta t = 0.25$ s earlier may be found from

$$\begin{aligned}\mathbf{u}'_{t-\Delta t} &= \mathbf{q}^*(-\Delta t)\,\mathbf{u}'_t\,\mathbf{q}(-\Delta t)\\ &= \mathbf{q}(\Delta t)\,\mathbf{u}'_t\,\mathbf{q}^*(\Delta t),\end{aligned}$$

where $\mathbf{q}(\Delta t) = \begin{bmatrix}\frac{\hat{\omega}_x}{\hat{\omega}}\sin(\Delta t\,\hat{\omega}/2) & \frac{\hat{\omega}_y}{\hat{\omega}}\sin(\Delta t\,\hat{\omega}/2) & \frac{\hat{\omega}_z}{\hat{\omega}}\sin(\Delta t\,\hat{\omega}/2) & \cos(\Delta t\,\hat{\omega}/2)\end{bmatrix}^{\mathrm{T}}$, and $\hat{\omega} = \sqrt{\hat{\omega}_x^2 + \hat{\omega}_y^2 + \hat{\omega}_z^2}$. To a good approximation, $\mathbf{q}(\Delta t) = \begin{bmatrix}\frac{\hat{\omega}_x\,\Delta t}{2} & \frac{\hat{\omega}_y\,\Delta t}{2} & \frac{\hat{\omega}_z\,\Delta t}{2} & 1\end{bmatrix}^{\mathrm{T}}$. Having amended the CCD distortion correction, the vectors are once again propagated forward by means of $\mathbf{u}'_t = \mathbf{q}^*(\Delta t)\,\mathbf{u}'_{t-\Delta t}\,\mathbf{q}(\Delta t)$.

available (up to 18) measurements were used and three cases were considered. In case (a) no back-propagation was performed; in case (b) measurements 1–9 were back-propagated whenever interlacing mode was active; and in case (c) measurements 10–18 were back-propagated whenever interlacing mode was active.[6] For this test the PACS scan map 1342236614 (OD 968) was used. Like the observation (1342254140) which was used to investigate the timing, this observation also contains a period, of approximately 80 s, when the attitude was changing rapidly ($\sim$ 375 ″/s). However, the advantage foreseen in using observation 1342236614 for this test is that it was made during a period of the mission for which the difference between the on-board and on-ground CCD distortion corrections is larger. One would therefore expect that the effect of amending the distortion correction at an erroneous point on the CCD would be more noticeable.

The resulting plots of the quality of the star tracker attitude determination, for the period when up to 18 stars were available, are shown in Figures 10–12. From this limited test, it appears that the effect of the back-propagation—even for a situation like this where it amounts to a movement of almost the width of one pixel on the CCD—is negligible. To facilitate further testing, an input parameter will be added to the software to allow either set of stars to be back-propagated.

It has been observed that, when estimating the star tracker attitude using just measurements 1–9, there is often a degradation of the quality for those periods when interlacing mode was active (see `HCSS-19398`). However, it is worth pointing out that this cannot be attributed to a failure to back-propagate the measurements. For example, for observation 1342250406 interlacing mode became active at around elapsed time 496.5 s and following this the quality of the star tracker attitude estimates created using measurements 1–9 is immediately degraded (Figure 13). However, immediately prior to elapsed time 483.5 s interlacing mode was also active and here the quality of the estimates made using stars 1–9 is very good. The situation is reversed for the attitude estimates created using measurements 10–18 (Figure 14). (Further evidence that the observed degradation in quality is not associated with the back-propagation is that it may also be seen in the attitude measurements created from the on-board star vectors, e.g. Figure 15.)

[6] Although the exact meaning of the interlacing flag, column `strmInterlacStatus` of the `AcmsScmTM` dataset, is not fully understood (see HCSS-18595), it was decided to assume that interlacing mode was active whenever this flag takes a non-zero value.

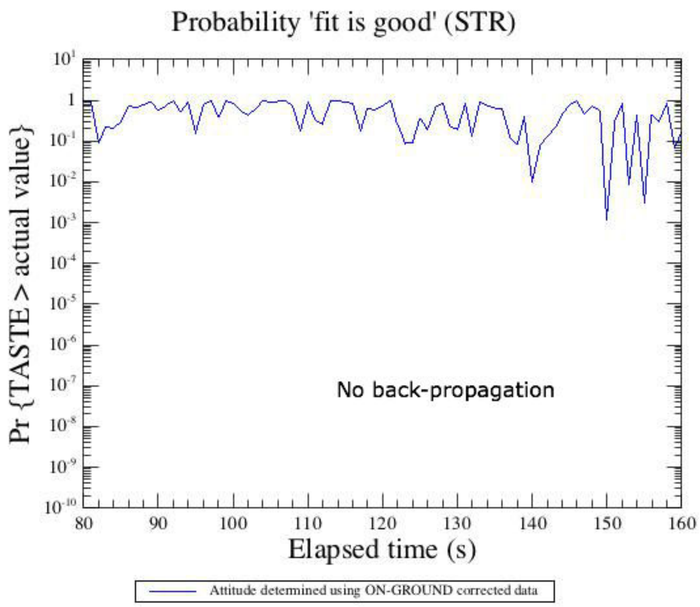


Figure 10: Attitude measurement quality (all stars, no back-propagation)

The explanation can be found in Figure 16, which shows that between these two periods when interlacing mode was active the two sets of stars (those in positions 1–9 and those in positions 10–18) exchange positions.[7] It appears therefore that, on average, either the measured or the catalogue positions of the stars originally in positions 1–9 are more accurate than those of the other stars.

[7]The exchange in positions is not perfect as during the first interlacing period star 1875 belongs to both sets, whereas during the second interlacing period star 2136 belongs to both sets.

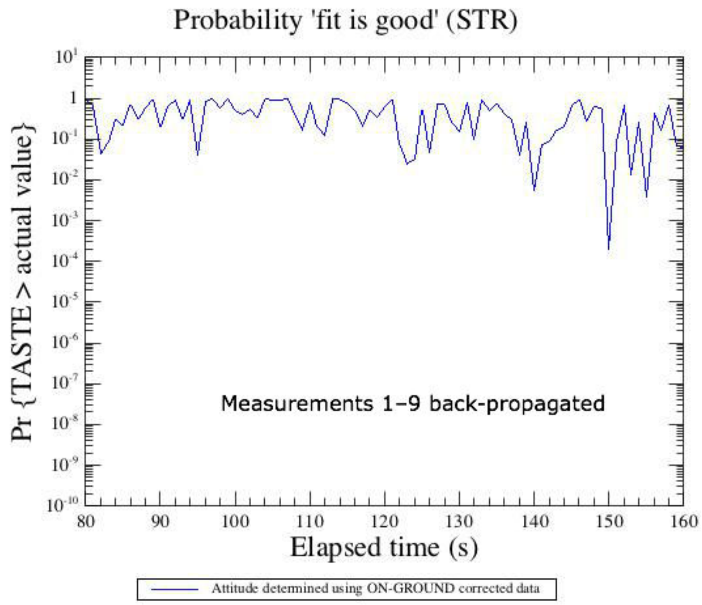


Figure 11: Attitude measurement quality (all stars, 1–9 back-propagated)

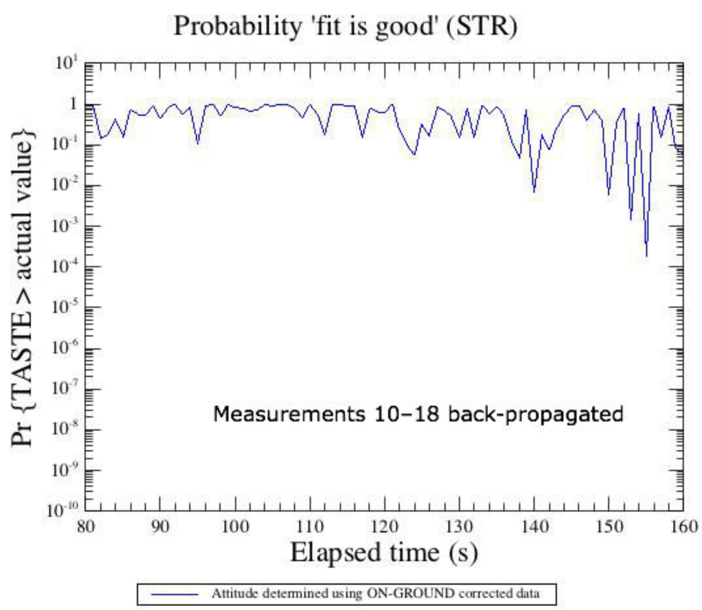


Figure 12: Attitude measurement quality (all stars, 10–18 back-propagated)

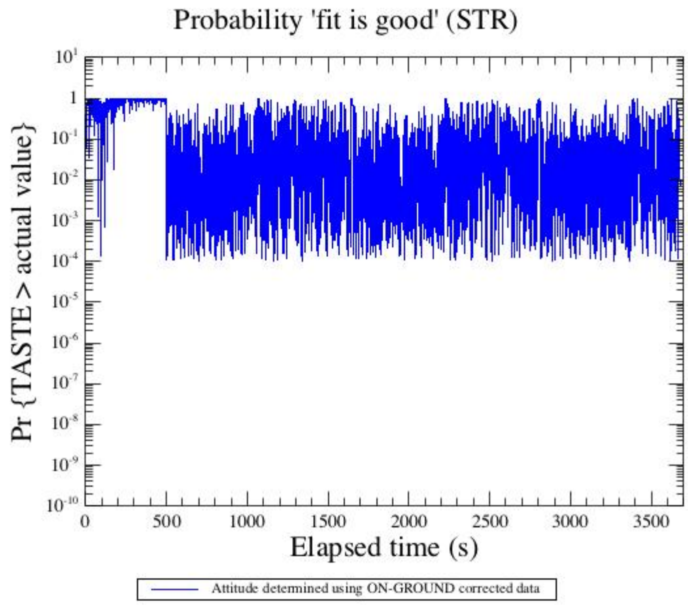


Figure 13: STR attitude measurement quality (stars 1–9)

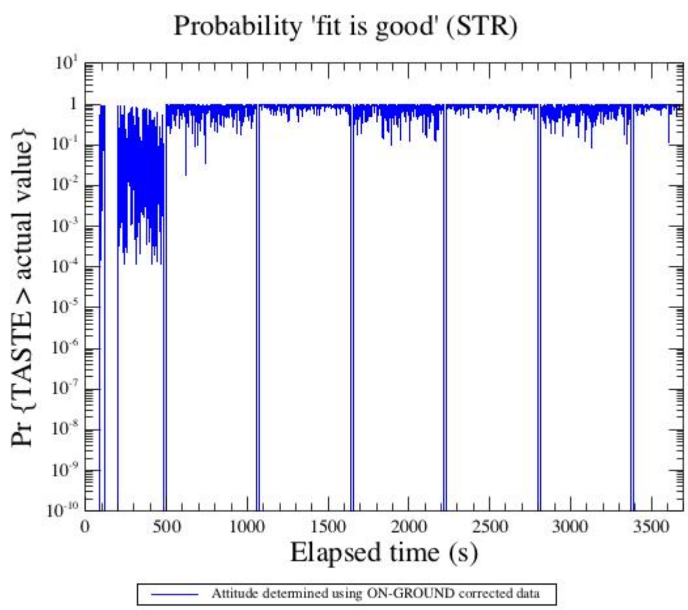


Figure 14: STR attitude measurement quality (stars 10–18)

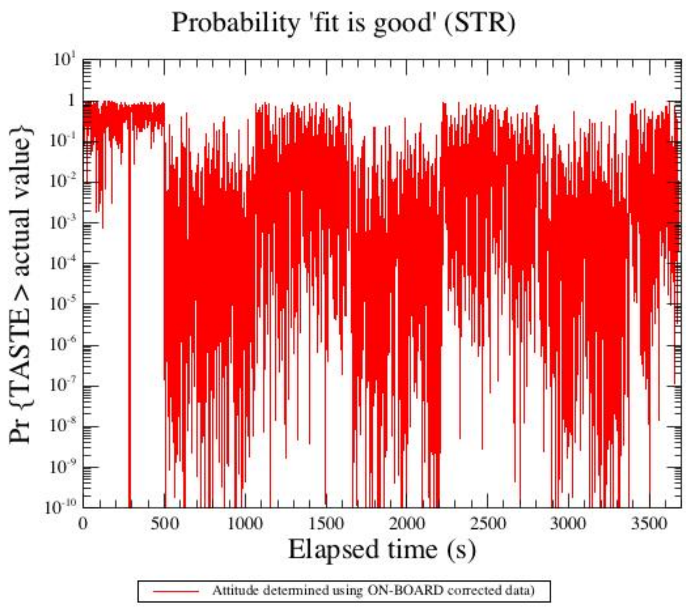


Figure 15: STR attitude measurement quality (stars 1–9, on-board vectors)

Table Data

| str01catId | str02catId | str03catId | str04catId | str05catId | str06catId | str07catId | str08catId | str09catId | str10catId | str11catId | str12catId | str13catId | str14catId | str15catId | str16catId | str17catId | str18catId | str |
|---|---|---|---|---|---|---|---|---|---|---|---|---|---|---|---|---|---|---|
| 2136 | 1829 | 2144 | 1928 | 1963 | 1874 | 1918 | 1959 | 1875 | 1785 | 1853 | 1870 | 65526 | 2086 | 2070 | 1919 | 2012 | 1875 | 25 |
| 2136 | 1829 | 2144 | 1928 | 1963 | 1874 | 1918 | 1959 | 1875 | 1785 | 1853 | 1870 | 65526 | 2086 | 2070 | 1919 | 2012 | 1875 | 25 |
| 2136 | 1829 | 2144 | 1928 | 1963 | 1874 | 1918 | 1959 | 1875 | 1785 | 1853 | 1870 | 65526 | 2086 | 2070 | 1919 | 2012 | 1875 | 25 |
| 2136 | 1829 | 2144 | 1928 | 1963 | 1874 | 1918 | 1959 | 1875 | 1785 | 1853 | 1870 | 65526 | 2086 | 2070 | 1919 | 2012 | 1875 | 25 |
| 2136 | 1829 | 2144 | 1928 | 1963 | 1874 | 1918 | 1959 | 1875 | 1785 | 1853 | 1870 | 65526 | 2086 | 2070 | 1919 | 2012 | 1875 | 25 |
| 2136 | 1829 | 2144 | 1928 | 1963 | 1874 | 1918 | 1959 | 1875 | 1785 | 1853 | 1870 | 65526 | 2086 | 2070 | 1919 | 2012 | 1875 | 25 |
| 2136 | 1829 | 2144 | 1928 | 1963 | 1874 | 1918 | 1959 | 1875 | 1785 | 1853 | 1870 | 65526 | 2086 | 2070 | 1919 | 2012 | 1875 | 25 |
| 2136 | 1829 | 2144 | 1928 | 1963 | 1874 | 1918 | 1959 | 1875 | 1785 | 1853 | 1870 | 65526 | 2086 | 2070 | 1919 | 2012 | 1875 | 25 |
| 2136 | 1829 | 2144 | 1928 | 1963 | 1874 | 1918 | 1959 | 1875 | 0 | 0 | 0 | 0 | 0 | 0 | 0 | 0 | 0 | 25 |
| 1875 | 2136 | 1829 | 2144 | 1928 | 1963 | 1874 | 1918 | 1959 | 0 | 0 | 0 | 0 | 0 | 0 | 0 | 0 | 0 | 27 |
| 1875 | 2136 | 1829 | 2144 | 1928 | 1963 | 1874 | 1918 | 1959 | 0 | 0 | 0 | 0 | 0 | 0 | 0 | 0 | 0 | 27 |
| 1875 | 2136 | 1829 | 2144 | 1928 | 1963 | 1874 | 1918 | 1959 | 0 | 0 | 0 | 0 | 0 | 0 | 0 | 0 | 0 | 27 |
| 1875 | 2136 | 1829 | 2144 | 1928 | 1963 | 1874 | 1918 | 1959 | 0 | 0 | 0 | 0 | 0 | 0 | 0 | 0 | 0 | 27 |
| 1875 | 2136 | 1829 | 2144 | 1928 | 1963 | 1874 | 1918 | 1959 | 0 | 0 | 0 | 0 | 0 | 0 | 0 | 0 | 0 | 27 |
| 1875 | 2136 | 1829 | 2144 | 1928 | 1963 | 1874 | 1918 | 1959 | 0 | 0 | 0 | 0 | 0 | 0 | 0 | 0 | 0 | 27 |
| 2136 | 1875 | 1829 | 2144 | 1928 | 1963 | 1874 | 1918 | 1959 | 0 | 0 | 0 | 0 | 0 | 0 | 0 | 0 | 0 | 25 |
| 2136 | 1875 | 1829 | 2144 | 1928 | 1963 | 1874 | 1918 | 1959 | 0 | 0 | 0 | 0 | 0 | 0 | 0 | 0 | 0 | 25 |
| 2136 | 1875 | 1829 | 2144 | 1928 | 1963 | 1874 | 1918 | 1959 | 0 | 0 | 0 | 0 | 0 | 0 | 0 | 0 | 0 | 25 |
| 2136 | 1875 | 1829 | 2144 | 1928 | 1963 | 1874 | 1918 | 1959 | 0 | 0 | 0 | 0 | 0 | 0 | 0 | 0 | 0 | 25 |
| 2136 | 1875 | 1829 | 2144 | 1928 | 1963 | 1874 | 1918 | 1959 | 0 | 0 | 0 | 0 | 0 | 0 | 0 | 0 | 0 | 25 |
| 1785 | 1853 | 1870 | 65526 | 2086 | 2070 | 1919 | 2012 | 2136 | 2136 | 1875 | 1829 | 2144 | 1928 | 1963 | 1874 | 1918 | 1959 | 26 |
| 1785 | 1853 | 1870 | 65526 | 2086 | 2070 | 1919 | 2012 | 2136 | 1875 | 1829 | 2144 | 1928 | 1963 | 1874 | 1918 | 1959 | 2136 | 26 |
| 1785 | 1853 | 1870 | 65526 | 2086 | 2070 | 1919 | 2012 | 2136 | 1875 | 1829 | 2144 | 1928 | 1963 | 1874 | 1918 | 1959 | 2136 | 26 |
| 1785 | 1853 | 1870 | 65526 | 2086 | 2070 | 1919 | 2012 | 2136 | 1875 | 1829 | 2144 | 1928 | 1963 | 1874 | 1918 | 1959 | 2136 | 26 |
| 1785 | 1853 | 1870 | 65526 | 2086 | 2070 | 1919 | 2012 | 2136 | 1875 | 1829 | 2144 | 1928 | 1963 | 1874 | 1918 | 1959 | 2136 | 26 |
| 1785 | 1853 | 1870 | 65526 | 2086 | 2070 | 1919 | 2012 | 2136 | 1875 | 1829 | 2144 | 1928 | 1963 | 1874 | 1918 | 1959 | 2136 | 26 |

Figure 16: 'Exchange' of positions within `AcmsDtmStr` dataset

# 4 Example and discussion

To illustrate the effect on the pointing reconstruction of using one set of star vector measurements or another we again look at the HIFI point mode DBS observation 1342250406 (i.e. the observation used for Figures 13–15).[8] Three cases were considered: (a) first set of measurements (i.e. stars 1–9); (b) second set of measurements (i.e. stars 10–18); and (c) all star measurements. The results (for elapsed time greater than 500 s) are shown in Figures 17–19.

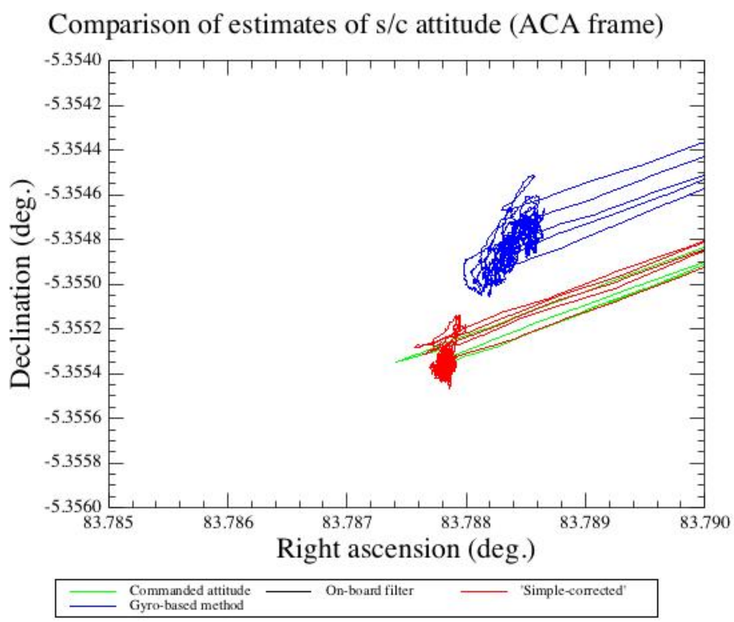


Figure 17: Observation 1342250406: (a) first set

## 4.1 Assignment of measurement errors

As discussed in [4, pp. 10–13], the estimation of the star tracker attitude makes use of the QUEST measurement model. That is, the error in each measured star vector, $\mathbf{u}'_i$, is modelled as a normally distributed random vari-

[8] 1342250406 is one of the observations considered in [3].

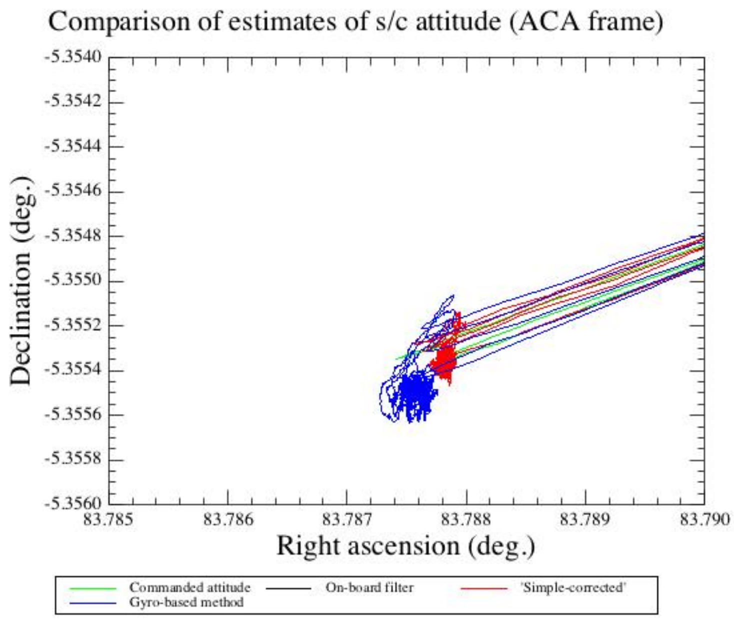


Figure 18: Observation 1342250406: (b) second set

able

$$\Delta \mathbf{u}'_i \sim N(\mathbf{0}, R_i),$$

which is assumed to lie perpendicular to the true direction, $\mathbf{u}'_{i,\mathrm{true}}$, and to have an axially-symmetric distribution with variance $\sigma_i^2$, i.e.

$$R_i = \sigma_i^2 (I_{3\times3} - \mathbf{u}'_{i,\mathrm{true}} \mathbf{u}'^{\mathrm{T}}_{i,\mathrm{true}}).$$

Moreover, a constant value, $\sigma = 2.9''$, is assumed for the standard deviation associated with each measurement and this value has been estimated from just a handful of observations (see `HCSS-19267`). That is, we are applying equal weight to each measurement.

However, earlier investigations—in which one measurement was removed at a time from the set used in the estimation—have demonstrated that the low $p$-values seen in Figure 13 (for values of the elapsed time greater than 500 s) are not caused by the presence of a single, or even by several, bad quality stars, but rather by the star vector measurements in this set of stars being, in general, less accurate than those in the other set. The most likely explanation is that the catalogue positions of these stars are simply less

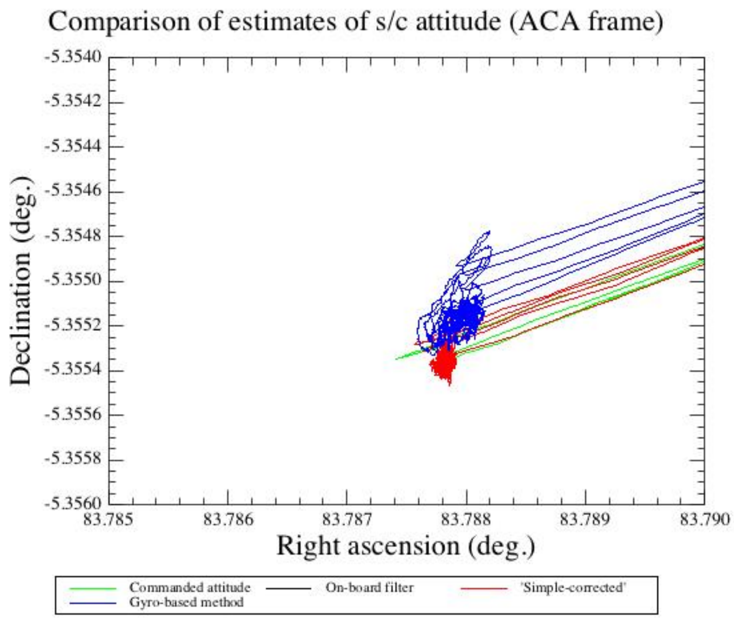


Figure 19: Observation 1342250406: (c) both sets

accurate. It appears that what we are seeing is a large variation in the accuracy associated with the various star vector measurements. The fact that we are applying equal weight to each measurement means that the star tracker attitude estimates we construct will not be optimal and that adding new measurements (using more stars) will not necessarily increase the accuracy of the final reconstructed attitude. For example, the (gyro-based) reconstructed attitude in Figure 18 may well be more accurate than that shown in Figure 19, despite the fact that fewer stars have been used. As noted in [1, p. 191], interlacing mode was only envisaged to increase the likelihood statistically of obtaining a more accurate result. There will be cases where using more stars degrades the accuracy.

Furthermore, if the above hypothesis that there is a sizeable error in the catalogue positions is true, then, since the same stars often remain in the field-of-view for long periods, the effect will be to produce a bias in the results and this bias cannot be reduced by simply using more measurements (increasing the parameter `wind_len`) in the least-squares fitting performed by `calcGyroAttitude`.

## 4.2 Goodness-of-fit

A further consequence of this variation in the accuracy of the star vector measurements is that, within the auxiliary processors, the attitudes reconstructed by the gyro-based method may be being rejected in favour of the 'simple-corrected' attitudes when there is nothing at all wrong with the (least-squares) fitting. That is, very low $p$-values may indicate simply that we are assuming an unrealistic value for the measurement error. The star tracker attitude measurements then appear to be of bad quality when, in fact, they are simply less accurate than expected.

A possible strategy for overcoming this might be along the lines of:

1. Modify the elimination of bad stars in `calcStrAttitude` so that a star is rejected based on the *relative* change in the TASTE variable (or the associated $p$-value) when it is excluded.

2. Once all bad stars have been excluded, assume that the $q$-method fit is good and re-estimate the measurement error using eq.(23) of [4, p. 13], with $N = 1$, i.e.

$$\widehat{\sigma} = \sigma_{\mathrm{ref}} \sqrt{\frac{\mathrm{TASTE}}{2n-3}}.$$

3. Use the new estimate of $\sigma$ to recompute the uncertainty in the star tracker attitude measurement.

4. Use these recomputed uncertainties when performing the least-squares fitting in `calcGyrAttitude`.

This strategy should lead both to a better reconstructed attitude (see Section 4.1) and to a more realistic $p$-value for testing the quality of the linear regression performed by `calcGyrAttitude`.

## 4.3 Repeated stars

It has been noticed that the same stars are often found in the two sets of interlacing mode data (e.g. Figure 20). Since it is recognized that any advantage associated with interlacing mode may be lost if the same stars are present in each ACMS cycle [1, p. 190], it may be worth ensuring that repeated stars are not used in the fitting.[9]

[9] Possibly the small advantage associated with having more measurements, even of the same stars, is offset by the error introduced by the forward-propagation.

Table Data

| str01catId | str02catId | str03catId | str04catId | str05catId | str06catId | str07catId | str08catId | str09catId | str10catId | str11catId | str12catId | str13catId | str14catId | str15catId | str16catId | str17catId | str18catId | str01Ra |
|---|---|---|---|---|---|---|---|---|---|---|---|---|---|---|---|---|---|---|
| 795 | 1159 | 877 | 925 | 1033 | 932 | 903 | 779 | 821 | 0 | 0 | 0 | 0 | 0 | 0 | 0 | 0 | 0 | 328.482 |
| 795 | 877 | 1159 | 925 | 1033 | 932 | 903 | 779 | 821 | 0 | 0 | 0 | 0 | 0 | 0 | 0 | 0 | 0 | 328.482 |
| 795 | 877 | 1159 | 925 | 1033 | 932 | 903 | 821 | 973 | 0 | 0 | 0 | 0 | 0 | 0 | 0 | 0 | 0 | 328.482 |
| 877 | 1159 | 925 | 1033 | 932 | 903 | 821 | 973 | 977 | 0 | 0 | 0 | 0 | 0 | 0 | 0 | 0 | 0 | 332.108 |
| 959 | 877 | 1159 | 925 | 1033 | 932 | 903 | 821 | 973 | 977 | 877 | 1159 | 925 | 1033 | 932 | 903 | 821 | 973 | 326.933 |
| 959 | 925 | 1159 | 1033 | 932 | 903 | 821 | 973 | 977 | 977 | 877 | 925 | 1159 | 1033 | 932 | 903 | 821 | 973 | 326.933 |
| 925 | 1159 | 1033 | 932 | 903 | 821 | 973 | 977 | 959 | 925 | 1159 | 1033 | 932 | 903 | 821 | 973 | 977 | 959 | 316.602 |
| 1175 | 959 | 1184 | 925 | 1159 | 1033 | 932 | 903 | 821 | 1184 | 925 | 1159 | 1033 | 932 | 903 | 821 | 973 | 977 | 320.752 |
| 959 | 1175 | 1184 | 925 | 1159 | 1033 | 932 | 903 | 973 | 973 | 977 | 1175 | 1184 | 925 | 1159 | 1033 | 932 | 903 | 326.933 |
| 959 | 1175 | 1184 | 925 | 1159 | 1033 | 932 | 903 | 973 | 977 | 1175 | 1184 | 925 | 1159 | 1033 | 932 | 903 | 973 | 326.933 |
| 959 | 1175 | 1184 | 925 | 1159 | 1033 | 932 | 903 | 973 | 977 | 1175 | 1184 | 925 | 1159 | 1033 | 932 | 903 | 973 | 326.933 |
| 973 | 959 | 1103 | 1175 | 1184 | 925 | 1159 | 1033 | 932 | 903 | 977 | 1103 | 1175 | 1184 | 925 | 1159 | 1033 | 932 | 316.504 |
| 973 | 959 | 1103 | 1175 | 1184 | 925 | 1159 | 1033 | 932 | 903 | 977 | 1103 | 1175 | 1184 | 925 | 1159 | 1033 | 932 | 316.504 |
| 973 | 959 | 1103 | 1175 | 1184 | 925 | 1159 | 1033 | 932 | 903 | 977 | 1103 | 1175 | 1184 | 925 | 1159 | 1033 | 932 | 316.504 |
| 973 | 959 | 1103 | 925 | 1175 | 1184 | 1159 | 1033 | 932 | 903 | 977 | 1103 | 1175 | 925 | 1184 | 1159 | 1033 | 932 | 316.504 |
| 973 | 959 | 1103 | 925 | 1175 | 1184 | 1159 | 1033 | 932 | 903 | 977 | 1103 | 925 | 1175 | 1184 | 1159 | 1033 | 932 | 316.504 |
| 973 | 959 | 1103 | 925 | 1175 | 1184 | 1159 | 932 | 1033 | 903 | 977 | 1103 | 925 | 1175 | 1184 | 1159 | 932 | 1033 | 316.504 |
| 973 | 959 | 1103 | 925 | 1175 | 1184 | 1159 | 932 | 903 | 903 | 977 | 1103 | 925 | 1175 | 1184 | 1159 | 932 | 1033 | 316.504 |
| 973 | 959 | 925 | 1103 | 1175 | 1184 | 1159 | 903 | 932 | 1033 | 977 | 1103 | 925 | 1175 | 1184 | 1159 | 932 | 903 | 316.504 |
| 973 | 959 | 925 | 1103 | 1175 | 1184 | 1159 | 903 | 932 | 1033 | 977 | 925 | 1103 | 1175 | 1184 | 1159 | 903 | 932 | 316.504 |
| 973 | 959 | 925 | 1103 | 1175 | 1184 | 1159 | 903 | 932 | 1033 | 977 | 925 | 1103 | 1175 | 1184 | 1159 | 903 | 932 | 316.504 |
| 932 | 973 | 959 | 1230 | 925 | 1103 | 1175 | 1184 | 1159 | 1230 | 1033 | 977 | 925 | 1103 | 1175 | 1184 | 1159 | 903 | 319.484 |
| 932 | 973 | 959 | 1230 | 925 | 1103 | 1175 | 1184 | 903 | 1159 | 1033 | 977 | 1230 | 925 | 1103 | 1175 | 1184 | 903 | 319.484 |
| 932 | 973 | 959 | 1230 | 925 | 1103 | 1175 | 1184 | 903 | 1159 | 1033 | 977 | 1230 | 925 | 1103 | 1175 | 1184 | 903 | 319.484 |
| 932 | 973 | 959 | 1230 | 925 | 1103 | 1175 | 1184 | 903 | 1159 | 1033 | 977 | 1230 | 925 | 1103 | 1175 | 1184 | 903 | 319.484 |
| 932 | 973 | 959 | 1230 | 925 | 1103 | 903 | 1175 | 1184 | 1159 | 1033 | 977 | 1230 | 925 | 1103 | 903 | 1175 | 1184 | 319.484 |
| 932 | 973 | 959 | 925 | 1230 | 1103 | 903 | 1175 | 1184 | 1159 | 1033 | 977 | 925 | 1230 | 1103 | 903 | 1175 | 1184 | 319.484 |
| 1184 | 973 | 959 | 925 | 1230 | 1103 | 903 | 932 | 1175 | 1159 | 1033 | 977 | 925 | 1230 | 1103 | 903 | 932 | 1175 | 321.666 |
| 1184 | 973 | 959 | 925 | 1230 | 903 | 1103 | 932 | 1175 | 1159 | 1033 | 977 | 925 | 1230 | 1103 | 903 | 932 | 1175 | 321.666 |
| 932 | 1184 | 973 | 959 | 1237 | 925 | 1230 | 903 | 1103 | 1175 | 1159 | 1033 | 977 | 1237 | 925 | 1230 | 903 | 1103 | 319.484 |
| 932 | 1184 | 973 | 959 | 1237 | 925 | 1230 | 903 | 1103 | 1175 | 1159 | 1033 | 977 | 1237 | 925 | 1230 | 903 | 1103 | 319.484 |

Figure 20: Repeated stars seen in observation 1342254140

# References

[1] ACMS Team (Dutch Space). Herschel-Planck ACMS User Manual. Technical Report H-P-4-DS-MA-001, Issue 4/4, Dutch Space, Feb 2009.

[2] G. Berrighi. ASTR for HERSCHEL/PLANCK User Manual. Technical Report H-P-4-GAF-MA-0001, Issue 7, Galileo Avionica, Oct 2006.

[3] P. Morris. Some Results from SPG 13 Product Validation using Pointing Products produced by calcAttitude. Jan 2015.

[4] C. Stephenson. Guide to the Herschel Gyro-based Attitude Reconstruction Software. Technical Report HERSCHEL-HSC-TN-2069, Issue 1.1, Herschel Science Centre, Jun 2015.